Article

Cell

HIV-1 Neutralizing Antibodies with Limited Hypermutation from an Infant

Graphical Abstract

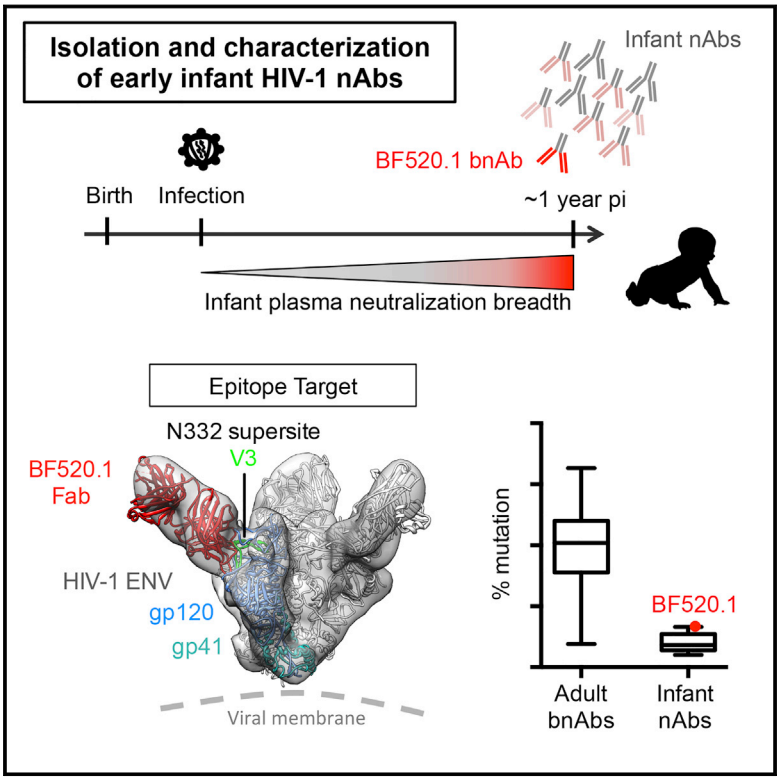

Authors

Cassandra A. Simonich, Katherine L. Williams, Hans P. Verkerke, James A. Williams, Ruth Nduati, Kelly K. Lee, Julie Overbaugh

Correspondence

joverbau@fredhutch.org

In Brief

Potent and broad neutralizing antibody responses to HIV typically take years to develop in infected adults, but new data in infected infants reveal a different pathway for their rapid development.

Highlights

- Infant HIV-1 nAbs isolated at ~1 year post-infection contribute to plasma breadth
- An infant broadly neutralizing antibody targets a known Env supersite
- Infant nAbs bind early transmitted Envs but do not neutralize corresponding virus
- Infant HIV-1 neutralizing antibodies have low levels of somatic hypermutation

Accession Numbers

KX159304–KX159315
KX168062–KX168123

Simonich et al., 2016, Cell *166*, 77–87
June 30, 2016
http://dx.doi.org/10.1016/j.cell.2016.05.055

CellPress

Cell

HIV-1 Neutralizing Antibodies with Limited Hypermutation from an Infant

Cassandra A. Simonich,[1,2] Katherine L. Williams,[1] Hans P. Verkerke,[3] James A. Williams,[3] Ruth Nduati,[4] Kelly K. Lee,[3] and Julie Overbaugh[1,2,*]

[1]Division of Human Biology, Fred Hutchinson Cancer Research Center, Seattle, WA 98109, USA
[2]Medical Scientist Training Program, University of Washington School of Medicine, Seattle, WA 98195, USA
[3]Department of Medicinal Chemistry, University of Washington, Seattle, WA 98195, USA
[4]Department of Pediatrics and Child Health, University of Nairobi, Nairobi, Kenya
*Correspondence: joverbau@fredhutch.org
http://dx.doi.org/10.1016/j.cell.2016.05.055

SUMMARY

HIV-1 broadly neutralizing antibodies (bnAbs) develop in a subset of infected adults and exhibit high levels of somatic hypermutation (SHM) due to years of affinity maturation. There is no precedent for eliciting highly mutated antibodies by vaccination, nor is it practical to wait years for a desired response. Infants develop broad responses early, which may suggest a more direct path to generating bnAbs. Here, we isolated ten neutralizing antibodies (nAbs) contributing to plasma breadth of an infant at ~1 year post-infection, including one with cross-clade breadth. The nAbs bind to envelope trimer from the transmitted virus, suggesting that this interaction may have initiated development of the infant nAbs. The infant cross-clade bnAb targets the N332 supersite on envelope but, unlike adult bnAbs targeting this site, lacks indels and has low SHM. The identification of this infant bnAb illustrates that HIV-1-specific neutralization breadth can develop without prolonged affinity maturation and extensive SHM.

INTRODUCTION

HIV-1 broadly neutralizing antibodies (bnAbs) are thought to be an important component of a protective HIV-1 vaccine but eliciting such responses remains elusive. Indeed, broad and potent neutralizing antibody responses are relatively rare even in HIV-infected individuals and typically take several years to develop, at least in adults where they have been most extensively studied (Mouquet, 2014). There have now been several detailed studies of adults who develop broad neutralizing antibody responses, with the goal of trying to reproduce this process with a vaccine, and a number of bnAbs have been isolated from chronic infection (Mascola and Haynes, 2013; West et al., 2014). Two recent studies showed these bnAbs can bind to virus that was transmitted, suggesting that an interaction with the infecting virus may have stimulated the germline B cell receptors (BCRs) to initiate development of the bnAb lineage (Doria-Rose et al., 2014; Liao et al., 2013).

Adult-derived bnAbs exhibit features reflective of long-term affinity maturation including high levels of somatic hypermutation (SHM) and rare insertions and deletions (indels) (Klein et al., 2013b; West et al., 2014). Longitudinal studies of bnAb development as well as studies examining predicted intermediates in this process demonstrated that the high degree of mutations and many indels are important for neutralization breadth and potency (Doria-Rose et al., 2014; Hoot et al., 2013; Kepler et al., 2014; Klein et al., 2013a; Kong et al., 2013; Liao et al., 2013; Scheid et al., 2011; Sok et al., 2013; Zhou et al., 2010). The unusual features of these bnAbs may be the result of a process of iterative rounds of affinity maturation in response to viral escape over years of infection before developing neutralization breadth (Klein et al., 2013b; West et al., 2014). While studies are underway to develop strategies to mimic this long-term process and guide affinity maturation (Doria-Rose and Joyce, 2015), this will undoubtedly be a challenging task.

HIV-1-infected infants were recently shown to produce plasma antibody responses that potently neutralize a diverse panel of HIV-1 isolates including more difficult to neutralize variants from across clades and these responses developed as early as 1–2 years post-infection (pi) (Goo et al., 2014). While adult HIV-1 bnAbs have been extensively characterized, nothing is known about infant bnAbs contributing to broad plasma responses. The relatively rapid development of infant plasma neutralization breadth may suggest that the bnAbs responsible for breadth have distinct features relative to adult HIV-1-specific bnAbs, including lower SHM. Furthermore, whether infant bnAbs target similar or novel epitopes on HIV-1 envelope (Env) compared to adult bnAbs is not known. To better understand the early development of bnAbs in natural infection, we isolated and characterized infant HIV-1-specific neutralizing monoclonal antibodies contributing to plasma breadth within the first year of infection.

RESULTS

Neutralizing Activity of Infant Plasma and Isolated Neutralizing Antibodies

Infant BF520 was HIV RNA- and DNA-negative at 8 days of age then subsequently detected positive at 114 days (3.8 months) of age, suggesting transmission likely occurred via breastfeeding. Plasma from this HIV-1 clade A infected infant demonstrated

			BF520 Plasma	BF520.1	BF520.2	BF520.3	BF520.4	BF520.5	BF520.6	BF520.7	BF520.8	BF520.9	BF520.10
		SIV	<100	>20	>20	>20	>20	>20	>20	>20	>20	>20	>20
Tier 1	Clade B	SF162	>3200	0.22	0.65	1.47	6.96	2.67	1.32	0.75	1.07	3.41	1.08
Tier 2	Clade A	Q461.d1	480	>20	1.72	1.76	6.23	>20	0.69	1.97	2.23	>20	>20
		Q23.17	339	0.29	>20	>20	>20	>20	>20	>20	>20	>20	>20
		Q842.d16	306	>50	25.7	19.5	26.7	11.4	>50	23	>50	42.1	>50
		Q769.B9	<100	>20	>20	>20	>20	>20	>20	>20	>20	>20	>20
		Q259.d2.26	121	>50	>50	>50	>40	>50	>50	>50	>50	>50	>50
		BJ613.E1	188	>50	>50	>50	>40	>50	>50	>50	>50	>50	>50
		Q168.a2	<100	>20	>20	>20	>20	>20	>20	>20	>20	>20	>20
		Q842.d12	115	>50	>50	>50	>40	>50	>50	>50	>50	>50	>50
	Clade A/D	BF535.A1	128	>50	>50	>50	>40	>50	>50	>50	>50	>50	>50
	Clade B	TRO.11	244	5.26	>20	>20	>20	>20	>20	>20	>20	>20	>20
		THRO4156.18	<100	>20	>20	>20	>20	>20	>20	>20	>20	>20	>20
		CAAN.A2	124	42.2	>50	>50	>20	>50	>50	>50	>50	>50	>50
Tier 3		TRJO4551.58	124	>20	>20	>20	>40	>20	>20	>20	>20	>20	>20
		PVO.4	119	38.1	>50	>50	>20	>50	>50	>50	>50	>50	>50
Tier 2	Clade C	ZMN109F.PB4	108	>20	>50	>50	>40	>50	>50	>50	>50	>50	>50
		QC406.F3	922	0.2	>20	>20	>20	>20	>20	>20	>20	>20	>20
		DU156.12	228	5.33	>20	>20	>20	>20	>20	>20	>20	>20	>20
		DU422.1	159	6.81	>50	>50	>20	>50	>50	>50	>50	>50	>50
		DU172.17	159	20.6	>50	>50	>20	>50	>50	>50	>50	>50	>50
		CAP210.E8	186	>20	>50	>50	>40	>50	>50	>50	>50	>50	>50
	Clade D	QB857.B3	142	>20	>50	>50	>40	>50	>50	>50	>50	>50	>50
		QD435.A4	110	>20	>50	>50	>40	>50	>50	>50	>50	>50	>50

Plasma IC_{50}

- IC_{50} >1000
- 500 ≤ IC_{50} < 1000
- 200 ≤ IC_{50} < 500
- 100 ≤ IC_{50} < 200
- IC_{50} < 100

mAb IC_{50} (μg ml^{-1})

- IC_{50} < 0.2
- 0.2 ≤ IC_{50} < 2
- 2 ≤ IC_{50} < 10
- 10 ≤ IC_{50} < 20-50
- IC_{50} >20-50

Figure 1. Neutralization of Panel Viruses with BF520 Plasma from 15 Months of Age and Isolated nAbs

IC_{50} values (μg ml^{-1}) are color coded with darker shading indicating greater neutralization potency. Gray shading indicates 50% neutralization was not achieved at the highest mAb concentration or lowest plasma dilution tested. SIV was a negative control. Values are an average of at least three independent experiments performed in duplicate.

cross-clade tier 2 neutralizing activity by as early as 12 months of age (Goo et al., 2014). IgG^+ memory B cells from 15 months of age, 11.2 months pi, were isolated and cultured. B cell culture supernatants were tested for neutralizing activity using a tier 1 clade B virus (SF162) and a tier 2 clade C virus (QC406.F3). These viruses were potently neutralized by BF520 plasma from the contemporaneous time point (IC_{50} > 3,200 and 922, respectively) (Goo et al., 2014). Ten antibodies with HIV-specific neutralizing activity were isolated and tested for neutralization against the cross-clade virus panel originally used to define the breadth of the infant plasma nAb response (Figure 1) (Goo et al., 2014). All isolated antibodies neutralized SF162; eight also neutralized either clade A heterologous tier 1 variant Q461.d1 or another clade A heterologous tier 2 virus Q842.d16 or both, indicating modest heterologous breadth specific to the clade of the infecting virus.

One infant antibody, BF520.1, neutralized tier 2 variants from clades A, B, and C and one tier 3 variant from clade B. Interestingly, this cross-clade bnAb did not neutralize some clade A variants that were neutralized by other isolated antibodies. Plasma neutralized eight viruses that were not neutralized by the isolated neutralizing antibodies (nAbs). However, plasma neutralization potency was low (IC_{50} < 200) for these eight viruses, suggesting the antibodies that drive this neutralization may be less potent and thus hard to identify with the functional screening approach used here. Thus, while antibody BF520.1 accounts for much of the plasma neutralization activity, the other nine nAbs we identified as well as additional unidentified antibodies contribute to overall breadth observed with BF520 plasma.

Breadth and Potency of Adult and Infant bnAbs

To compare the neutralizing activity of BF520.1 to adult bnAbs, we tested for neutralization of a global panel of viruses designed for standardized assessments of nAbs (Figure 2) (deCamp et al., 2014). BF520 plasma from 15 months of age neutralized 10/12 of the virus panel. BF520.1 neutralized 7/10 viruses neutralized by the corresponding plasma. Only one of the other nine nAbs neutralized a virus from this panel (virus 398F1, nAb BF520.4; IC_{50} = 14 μg ml^{-1}). We compared BF520.1 to first-generation adult bnAbs, which have moderate breadth and potency, and

			V3 glycan	Outer domain glycan	V3 glycans	CD4bs		V1/V2 glycans		gp120-gp41 interface	MPER		
		BF520 Plasma	**BF520.1**	**2G12**	**PGT121**	**b12**	**VRC01**	**PG16**	**PGT145**	**PGT151**	**4E10**	**2F5**	**10E8**
Clade A	398F1	527	0.47	>20	<0.02	2.4	0.44	>20	>20	<0.02	>20	4.76	0.81
Clade B	TRO11	175	4.92	2.75	0.03	>20	3.08	16	0.37	>20	6.74	>20	0.08
	X2278	183	1.19	2.14	<0.02	>20	0.63	<0.02	<0.02	2.21	>20	16.0	1.37
CRF07_BC	BJOX002000	159	0.62	>20	<0.02	>20	>20	<0.02	>20	<0.02	16.8	>20	1.37
	CH119	122	5.48	>20	<0.02	>20	7.15	10.3	2.94	>20	>20	>20	3.84
	CE1176	118	4.59	>20	<0.02	>20	17.8	<0.02	>20	<0.02	>20	>20	0.99
Clade C	CE0217	107	2.49	>20	<0.02	>20	1.68	<0.02	0.29	>20	12.9	>20	2.09
	25710	120	>20	>20	<0.02	>20	5.37	<0.02	<0.02	>20	4.98	>20	0.09
Clade G	X1632	116	>20	>20	>20	>20	0.35	0.26	2.24	>20	15.7	8.76	2.29
CRF01_AE	CNE55	113	>20	>20	>20	>20	2.2	17.3	<0.02	>20	>20	6.29	0.28
	CNE8	>100	>20	>20	>20	>20	3.86	3.16	1.29	>20	10.6	4.46	1.01
AC recomb	246F3	>100	>20	>20	>20	>20	1.44	<0.02	>20	8.56	>20	5.58	1.91
% Breadth		83	58	17	67	8	92	92	67	42	50	50	100
geometric mean IC_{50} (μg ml^{-1}) viruses neutralized			1.95	2.43	0.02	2.4	2.13	0.24	0.23	0.17	10.3	6.86	0.82
geometric mean IC_{50} (μg ml^{-1}) all viruses			5.14	14.1	0.35	16.8	2.57	0.35	1.01	2.76	14.4	11.7	0.82

Plasma IC_{50}

- IC_{50} >1000
- 500 ≤ IC_{50} < 1000
- 200 ≤ IC_{50} < 500
- 100 ≤ IC_{50} < 200
- IC_{50} < 100

mAb IC_{50} (μg ml^{-1})

- IC_{50} < 0.2
- 0.2 ≤ IC_{50} < 2
- 2 ≤ IC_{50} < 10
- 10 ≤ IC_{50} < 20
- IC_{50} >20

Figure 2. Comparison of BF520.1 to Adult bnAbs

Neutralization of global panel tier 2 viruses. mAb IC_{50} values are an average of two to three independent experiments performed in duplicate. First-generation bnAbs indicated in gray.

a selection of broad and potent second-generation adult bnAbs (Falkowska et al., 2014; West et al., 2014). The neutralization breadth of BF520.1 (58%; Figure 2) is greater than that of the first-generation adult bnAbs, which range from 8%–50%, and falls within the range for the second-generation adult bnAbs (42%–100%). BF520.1 also demonstrates greater neutralization potency (geometric mean IC_{50} for viruses neutralized = 1.95 μg ml^{-1}; Figure 2) compared to first-generation adult bnAbs (2.4–10.3 μg ml^{-1}) and has comparable potency to the CD4 binding site directed bnAb VRC01 (2.13 μg ml^{-1}) (Wu et al., 2010), which is actively being pursued in rational vaccine design and tested for efficacy in human trials (Jardine et al., 2015; Lynch et al., 2015). Overall, these data from the global reference panel show that the infant bnAb BF520.1 demonstrates generally similar neutralization breadth to many adult bnAbs but with lower potency.

Epitope Specificity of BF520.1

The infant cross-clade bnAb BF520.1 exhibited a similar neutralization profile to the PGT-class of bnAbs (Goo et al., 2012a), which target the N332 glycan in V3 (Walker et al., 2011). Thus, we examined the effect of N332 on BF520.1 neutralization (Figures 3A and 3B). Neutralization was disrupted by removal of the N332 glycan for two viruses tested (93- and 5-fold increase IC_{50}), similar to what was observed for a prototype N332-directed bnAb, PGT128 (32- and 17-fold increase IC_{50}). Adding the N332 glycan to an infant clade A heterologous virus BG505.W6.C2 (Wu et al., 2006) resulted in increased neutralization sensitivity (17-fold decrease IC_{50}). These data indicate that this infant antibody targets a similar site on Env as the N332-dependent adult nAbs such as 2G12 and the PGT class of adult bnAbs (Kong et al., 2013; Mouquet et al., 2012; Pejchal et al., 2011; Scanlan et al., 2002; Trkola et al., 1996; Walker et al., 2011). Single-particle negative-stain electron microscopy (EM) analysis of Fab from the BF520.1 bnAb complexed with BG505.W6.C2.T332N SOSIP trimers, which encodes N332 and is structurally similar to Env on virus particles (Sanders et al., 2013), confirmed that the antibody targets the base of the V3 loop (Figure 3C). BF520.1 and PGT128 appear to dock to the trimer at the base of V3 with an overlapping footprint and to be oriented relative to the trimer with a similar angle of approach (Lee et al., 2015; Pejchal et al., 2011). The BF520.1 Fab, however, is slightly twisted and docked more closely to the gp120 core than PGT128 (Figure S1). At the resolution of the negative-stain reconstruction we are not able to infer the role of the complementarity determining region (CDR) loops or the specific residues on the paratope or epitope that are involved in this interaction. Thus, while our mutagenesis data implicates the glycan at N332 is an important component of the epitope for BF520.1, additional studies are needed to more directly compare the BF520.1 epitope and paratope to those of other antibodies that target the N332 supersite.

Binding to Autologous and Heterologous HIV-1 Envelopes

To gain insight into the development of the isolated infant antibodies, we examined whether the infant nAbs bind and/or

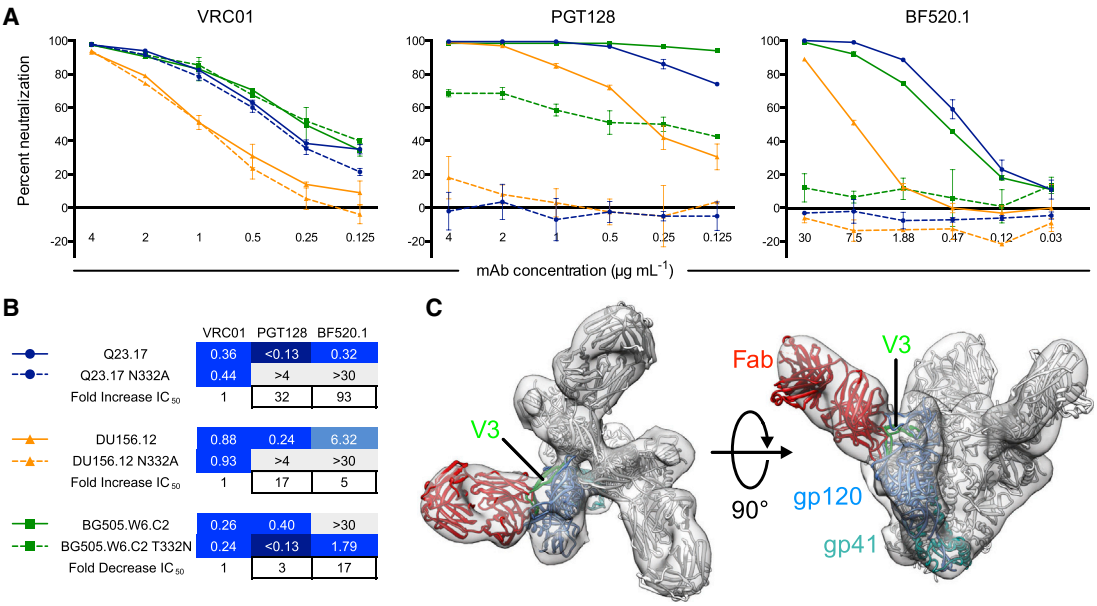

Figure 3. Epitope Mapping of BF520.1

(A and B) mAb neutralization of Q23.17 and DU156.12 wild-type viruses relative mutant viruses lacking the N332 glycan and BG505.W6.C2 relative to a mutant virus with N332 (T332N). PGT128 and VRC01 are positive and negative controls, respectively. Viruses lacking N332 are indicated by dashed lines.

(C) Negative-stain EM of the BG505.W6.C2.T332N SOSIP trimer in complex with BF520.1 Fab.

See also Figure S1.

neutralize autologous Env variants isolated at first HIV detection (3.8 months/14 weeks of age, designated "W14"). The diversity among these Env variants was low (maximum pairwise distance = 0.0067; Figure S2). Surprisingly, all 10 nAbs failed to neutralize the 11 early-stage, transmitted variants, despite potent neutralization by contemporaneous plasma (Figure S3), suggesting our functional screen for heterologous neutralization did not capture the nAbs mediating autologous neutralization by plasma from the 15-month time point. Despite the lack of neutralization of the earliest isolated variants, BF520.1 and the other nine infant nAbs bound to the corresponding autologous BF520.W14 cell-surface Env variants (Figure 4). Each of the ten infant nAbs also bound SF162, which they all neutralized, with BF520.1 exhibiting the highest level of binding, comparable to that of VRC01 (Figure 4).

Because it is unexpected that antibodies that bind Env trimer expressed natively on the cell surface would not neutralize the corresponding virus (Burton and Mascola, 2015; Fouts et al., 1997; Parren et al., 1998; Yasmeen et al., 2014), we sought to validate the flow cytometry analysis of antibody binding by measuring binding of the BF520 antibodies to BF520 native-like SOSIP trimer based on the BF520.W14.E3 transmitted Env variant. The purity of the native-like BF520 SOSIP trimer preparation was confirmed by SDS-PAGE, BN-PAGE and dynamic light scattering (Figure S4). Biolayer interferometry (BLI) demonstrated that all ten infant nAbs bound tightly to the BF520 SOSIP trimer representing the transmitted virus (Figure 5). To address whether avidity contributes to the observed binding kinetics, we measured Fab fragment binding to BF520 SOSIP trimer for representative nAbs. Purity and size of Fab fragments was confirmed for six of the infant nAbs by SDS-PAGE and mass spectrometry including the infant bnAb BF520.1. These Fabs bound to the autologous trimer with lower affinity compared to IgG for five of six Fabs tested and comparable affinity for one of six Fabs (Figure S5).

To compare infant bnAb BF520.1 binding to the early autologous variant with binding to heterologous envelope variants, we again assessed binding to cell-surface expressed Env by flow cytometry and to SOSIP trimers by BLI. The envelopes derived from heterologous viruses that were neutralized by the BF520.1 antibody (SF162, Q23.17, and BG505.W6.C2.T332N; Figure 6A) showed strong antibody binding (Figure 6B), and those that were not neutralized (BG505.W6.C2 and the related maternal-derived MG505.W0.E1 Env, both of which lack N332 [Wu et al., 2006]; Figure 6A) did not show binding to cell surface expressed Env (Figure 6B). Similar binding results were observed with the soluble SOSIP trimers for BG505.W6.C2, MG505.W0.E1, and BG505.W6.C2.T332N (Figure 6C). While binding by BF520.1 to BG505.W6.C2 soluble SOSIP trimer was detected by BLI, a high off-rate was observed (Figure 6C). Again, BF520.1 binding was detected to both the surface expressed and soluble forms of the BF520.1 Env trimer with a K_d of 8 nM.

To determine whether the infant bnAb, BF520.1 neutralizes later autologous viruses, Env variants were isolated from 2.2 months after the first, early, transmitted viral sequences were obtained (6 months of age, designated "M6"; Figure S2), which was 9 months prior to the time the nAbs were obtained. BF520.1 demonstrated potent neutralization of three of seven viruses from this time point (Figure S6).

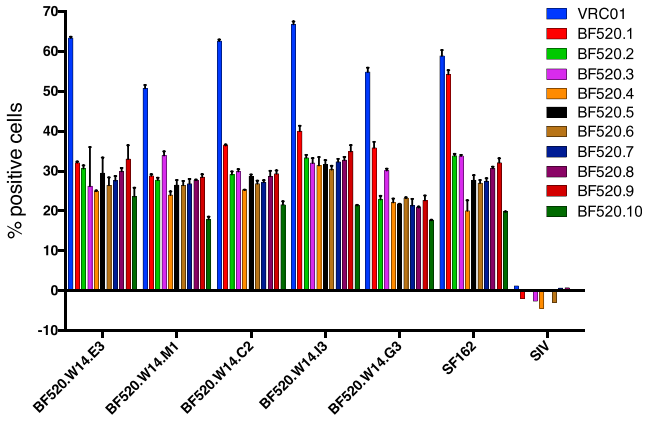

Figure 4. mAb Binding to Cell-Surface-Expressed Autologous HIV Envs from the Time Point When Infection Was First Detected, Week 14

Infant nAb binding to representative BF520 cell-surface expressed Env variants detected by flow cytometry as percentage of cells positive for bound antibody with background subtracted (mAb binding to mock transfected cells). VRC01 was included as a positive control for Env expression. SIV was included as a negative control. Data are representative of two independent experiments performed in duplicate. Error bars indicate SD based on duplicates within an experiment.

See also Figure S2.

Sequence Characteristics of Infant versus Adult bnAbs

The ten infant antibodies have different heavy chain gene rearrangements and CDRH3 sequences (Figure S7A) suggesting that they are produced from distinct lineages of B cells. Because these antibodies developed within 1 year pi, we were interested in examining the level of SHM of isolated infant-derived nAbs compared to adult bnAbs. All infant nAbs had low SHM (2.0%–6.6% at the nucleotide [nt] level; Figures 7A and S7), in contrast to adult bnAbs (3.8%–32.6% nt) (Eroshkin et al., 2014; Lefranc et al., 2009) as well as adult nAbs with limited tier 2 neutralizing activity (tier 1 nAbs; 2.4%–18.6% nt) (Li et al., 2015). The infant nAbs also had lower SHM than adult nAbs, including those with and without breadth, isolated relatively early pi (1–4 years) from CAP256-VRC26 (4.2%–18% nt) (Doria-Rose et al., 2014, 2015). Overall, infant HIV-specific nAbs are remarkable for the low level of SHM compared to adult nAbs.

BF520.1 had a much lower level of mutation (6.6% nt) compared to adult N332-dependent bnAbs (15.8%–23.1% nt) (Figures 7A and 7B). This infant bnAb was also notable when compared to adult bnAbs targeting the N332 supersite in that it lacks heavy and light chain indels (Figure 7B). BF520.1 has a CDRH3 of 20 amino acids, comparable to the PGT bnAbs (20–26 amino acids), but different heavy chain VDJ and light chain VJ gene rearrangements than the adult N332 bnAbs (Figure 7B) (Kunert et al., 1998; Trkola et al., 1996; Walker et al., 2011; Yu and Guan, 2014).

DISCUSSION

Adult bnAbs identified to date were isolated from chronically infected adults from as early as 2 to over 15 years post-infection (Doria-Rose et al., 2014; Wu et al., 2010). Longitudinal studies of bnAb development suggest these antibodies undergo iterative rounds of SHM and affinity maturation over years of infection before developing neutralization breadth (West et al., 2014). Characterizing bnAbs that develop early in natural infection will be important to help design vaccine strategies to elicit these antibodies over a shorter period of time. In this study, we successfully isolated infant nAbs contributing to plasma neutralization breadth at ~1 year pi. These infant nAbs exhibit low levels of SHM compared to adult nAbs suggesting that HIV-1-specific neutralization breadth can develop without the requirement for several years of antibody affinity maturation. Moreover, they suggest that infants may provide unique insights into optimal pathways to develop HIV-1-specific bnAbs.

Adult bnAbs target a number of conserved sites of vulnerability on the HIV-1 Env trimer (Wibmer et al., 2015). Here, we identified an infant bnAb targeting one of these known epitopes, the glycan-dependent N332 supersite. BF520.1 neutralization is dependent on the N332-glycan and the antibody binds the base of the V3 loop. bnAb responses targeting the N332 supersite are of particular interest for vaccine design as they are one of the most commonly found bnAb responses (Landais et al., 2016). However, the high levels of SHM seen in adult N332-dependent bnAbs present significant challenges as vaccine-elicited HIV-specific antibodies in humans exhibit much lower levels (0% to 8.2% V_H mutation) (Moody et al., 2012). BF520.1 falls within this range and overall shows better breadth and potency for this level of SHM compared to less mutated lineage variants of adult bnAb PGT121 (Sok et al., 2013) as well as the MPER-directed adult bnAb M66.6 (Zhu et al., 2011), which has the lowest level of SHM among adult bnAbs (Figure 7; indicated in purple). In addition, the PGT lineage antibodies have indels (Walker et al., 2011) that are important for neutralization (Kong et al., 2013; Sok et al., 2013), and BF520.1 lacks these rare insertions and deletions, which may simplify eliciting this response by vaccination. Another characteristic of glycan-targeting bnAbs is a long CDRH3 loop that reaches through the glycan shield and contacts the protein surface of Env (Kong et al., 2013; Pejchal et al., 2011). While BF520.1 has the critical long loop structure, it utilizes distinct V and J heavy chain genes as well as different heavy and light chain gene rearrangements compared to other N332-dependent bnAbs (Yu and Guan, 2014) suggesting there are multiple pathways that can lead to the development of these glycan-dependent bnAbs.

We found that the nAbs isolated at ~1 year pi bound to Env trimer of the transmitted virus. However, these nAbs do not neutralize the corresponding virus, although they neutralize heterologous viruses. For HIV-1-specific bnAbs isolated to date, there is usually a strong linkage between trimer binding and neutralization (Burton and Mascola, 2015; Fouts et al., 1997; Parren et al., 1998; Yasmeen et al., 2014). Lower affinity binding by Fab fragments compared to IgG for some infant nAbs suggests avidity effects may contribute to the strong binding for IgG and may account for the lack of neutralization of early autologous virus exhibited by some of the isolated nAbs. However, BF520.10 Fab fragments bound with comparable affinity as IgG to native-like soluble trimer of the autologous virus yet it did not neutralize

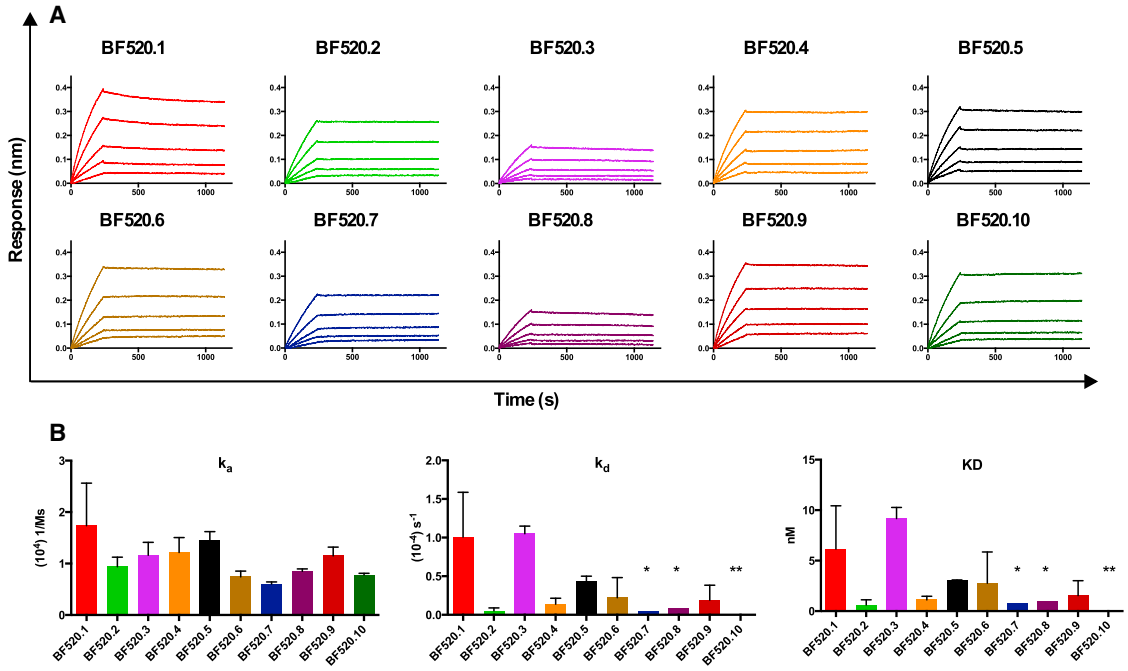

Figure 5. Infant nAb Binding to BF520.W14.E3 Native-like SOSIP Trimer

(A) Representative reference-subtracted sensor grams for each interaction between an infant nAb and the autologous SOSIP. Analyte concentrations range from 500 nM to 31.25 nM.

(B) Summarized affinity, association, and dissociation parameters (KD, ka, and kd, respectively) from best fitting to a 1:1 model of ligand:analyte binding are shown. Each parameter represents the average of two or three independent experiments unless otherwise indicated. Error bars indicate the SEM. *Minimal dissociation could only be fit to one replicate. **No dissociation after 30 min.

See also Figures S3, S4, S5, and S6.

the corresponding virus. Furthermore, all ten infant nAbs bound to cell-surface expressed Env variants from the early virus. Thus, this seems to represent a case in which antibodies that were capable of binding specifically to native Env of the early autologous virus were elicited but lacked the ability to neutralize the corresponding virus. The BF520.1 bnAb does neutralize autologous virus from 2.2 months later, which was 9 months prior to when the nAbs were isolated. Thus, one model for these data is that the binding interaction of the BCRs with the autologous transmitted Env antigen may have initiated the maturation of these antibodies and subsequent responses to the evolving virus led to selection of B cells expressing nAbs. Studies of the infant BCR repertoire prior to and over the course of infection will be needed to test this model and to more precisely define the progenitor BCRs for these nAbs.

It is unclear how infants develop bnAbs, although high viral load has been implicated (Goo et al., 2014). Furthermore, it is not known whether the lower levels of SHM seen for these infant antibodies is a result of inherent limitations of early-life B cell responses. However, infant B cell responses can exhibit adult-like diversity and SHM before 1 year of age (Siegrist and Aspinall, 2009), and there are unique features of mother-infant transmission that may also contribute to the rapid development of these responses. For example, passively acquired maternal antibodies present in infant circulation at the time of HIV-1 exposure may be playing a role by augmenting de novo nAb responses, as suggested by studies of macaques (Haigwood et al., 2004; Ng et al., 2010). In addition, passively acquired antibodies may shape the epitopes exposed on vertically transmitted variants as maternal antibody escape variants are transmitted to infants (Goo et al., 2012b; Wu et al., 2006). Relevant to this, an infant envelope variant shows promise as an immunogen (Sanders et al., 2015). Given that BF520.1 binds the Env of the transmitted variant, these findings raise the possibility that using Env immunogens based on vertically transmitted variants, possibly along with passively administered HIV-1-specific nAbs, may elicit antibodies similar to those identified here. In addition, this study, while only of a single infant, provides strong rationale to characterize nAbs from additional infants to determine the ontogeny of infant nAb responses and whether infant bnAbs generally have low levels of SHM.

In summary, we have isolated HIV-1-specific neutralizing antibodies from an infant who developed plasma cross-clade neutralization by 1-year pi. One of these demonstrates broad neutralization and has unique features compared to adult bnAbs targeting the same N332 supersite including low SHM, a lack of indels, and distinct germline gene usage. Moreover, this bnAb can bind the transmitted viral Env trimer but does not neutralize the virus, another unique feature compared to other described HIV bnAbs. Overall, the identification of an infant bnAb that developed early and has low SHM is encouraging for vaccine development. Specifically, BF520.1 may provide a template for glycan-dependent bnAbs that require limited SHM and thus may be relevant to studies to define immunization strategies to

A

	Neutralization IC_{50} (μg ml^{-1})			
	PGT128	VRC01	BF520.1	PGT145
SF162	<0.31	1.12	0.22	>20
BF520.W14.E3	0.13	<0.63	>20	>20
BG505.W6.C2	0.40	0.26	>30	<0.63
BG505.W6.T332N	<0.13	0.24	1.79	<0.63
MG505.W0.E1	>20	<0.63	>30	<0.63
Q23	<0.02	0.22	0.29	>20
SIV	>20	>20	>20	>20

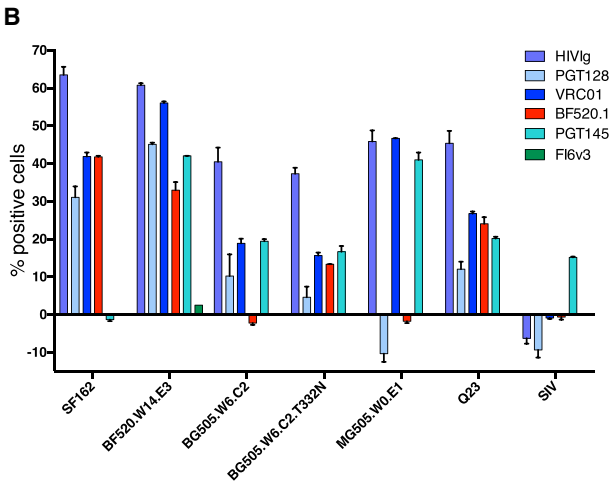

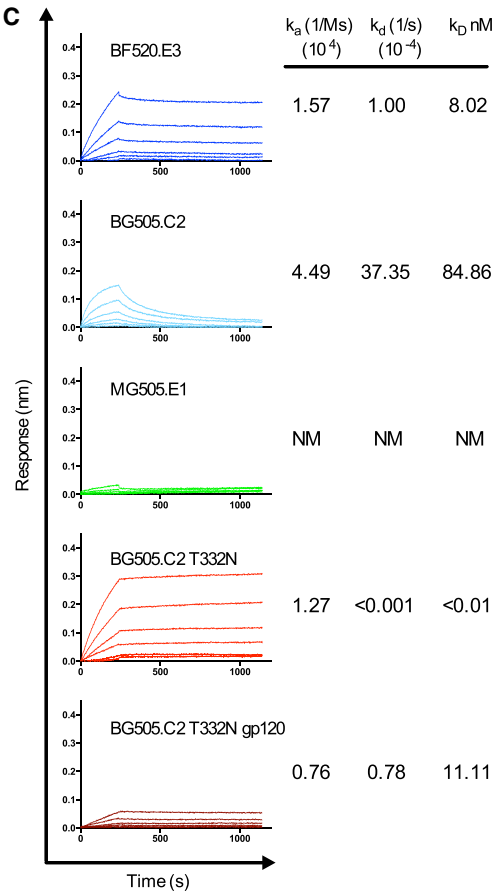

	k_a (1/Ms) (10^4)	k_d (1/s) (10^{-4})	k_D nM
BF520.E3	1.57	1.00	8.02
BG505.C2	4.49	37.35	84.86
MG505.E1	NM	NM	NM
BG505.C2 T332N	1.27	<0.001	<0.01
BG505.C2 T332N gp120	0.76	0.78	11.11

Figure 6. Binding and Neutralization of Heterologous Envs

(A) Neutralization IC_{50} values (μg ml^{-1}) for mAb neutralization of the corresponding virus. Values are an average of two independent experiments.

(B) mAb binding to cell-surface Env detected by flow cytometry. FI6v3 was an influenza-specific negative control. HIVIg was a positive control for Env expression. Data are representative of two independent experiments performed in duplicate. Error bars indicate SD based on duplicates within an experiment.

(C) BF520.1 binding to native-like soluble SOSIP trimers measured by BLI. NM, not modeled.

See also Figures S3, S4, S5, and S6.

elicit such bnAbs without the requirement for a long-term maturation pathway.

EXPERIMENTAL PROCEDURES

Infant Plasma and Peripheral Blood Mononuclear Cell Samples

Plasma and peripheral blood mononuclear cell (PBMC) samples were from infant BF520 enrolled in the Nairobi Breastfeeding Clinical Trial (Nduati et al., 2000), which was conducted prior to the use of antiretrovirals for prevention of mother-to-child transmission. Approval to conduct the Nairobi Breastfeeding Clinical Trial was provided by the ethical review committee of the Kenyatta National Hospital Institutional Review Board, the Fred Hutchinson Cancer Research Center Institutional Review Board, and the University of Washington Institutional Review Board.

BF520 was HIV-1 DNA-negative by PCR and HIV-1 RNA-negative using the Gen-Probe HIV-1 Viral Load assay at 8 days of age and was HIV-1 DNA- and RNA-positive by 3.8 months of age. Time pi was defined as the time from the infant's first HIV-1-positive nucleic acid test (3.8 months of age).

Sorting of B Cells and Reconstruction of Antibodies

HIV-specific B cells were identified using culture of IgG$^+$ B cells with subsequent neutralization assays of individual culture supernatants (Huang et al., 2013). A PBMC sample from BF520 from 15 months of age, 11.2 months pi, was thawed at 37°C and re-suspended in 10 ml B cell media (IMDM medium, GIBCO; 10% low IgG FBS, Life Technologies; 5 ml GlutaMAX, Life Technologies; 1 ml MycoZap plus PR, Lonza) plus 20 μl benzonase followed by centrifugation at 300 × *g* for 10 min. Cells were washed in FACS wash (1× PBS, 2% FBS) and stained on ice for 30 min using a cocktail of anti-CD19-BV510, anti-IgD-FITC, anti-IgM-FITC, anti-IgA-FITC, anti-CD3-BV711, anti-CD14-BV711, and anti-CD16-BV711. Cells were then washed once and resuspended in fluorescence-activated cell sorting (FACS) wash. Cells were loaded onto a BD FACS Aria II cell sorter, and IgG expressing B cells were identified as CD3$^-$CD14$^-$CD16$^-$CD19$^+$IgD$^-$IgM$^-$IgA$^-$ cells. The PBMC sample contained ~10 million cells with 72% viability. In total, ~100,000 IgG$^+$ B cells were sorted into B cell media. Cells were plated using a Tecan automated liquid handling system at a density of 6 B cells in 60 μl per well into 55 × 384-well plates in B cell media containing 100 U ml^{-1} IL-2 (Roche), 0.05 μg ml^{-1} IL-21 (Invitrogen), and 8.85 × 10^5 ml^{-1} irradiated 3T3/CD40L feeder cells (kindly provided by S. Riddell, FHCRC). After 14 days of incubation, IgG was detected by ELISA in 81% of a random sample of wells at a concentration of >10 ng ml^{-1} and 54% at >100 ng ml^{-1}.

B cell culture supernatant from each well was divided into 2 × 384-well plates at 20 μl each for neutralization assays using a Tecan automated liquid handling system. B cells were frozen at −80°C in 20 μl RNA storage buffer per well (15 mM Tris and 10 U murine RNase inhibitor, NEB). For each well,

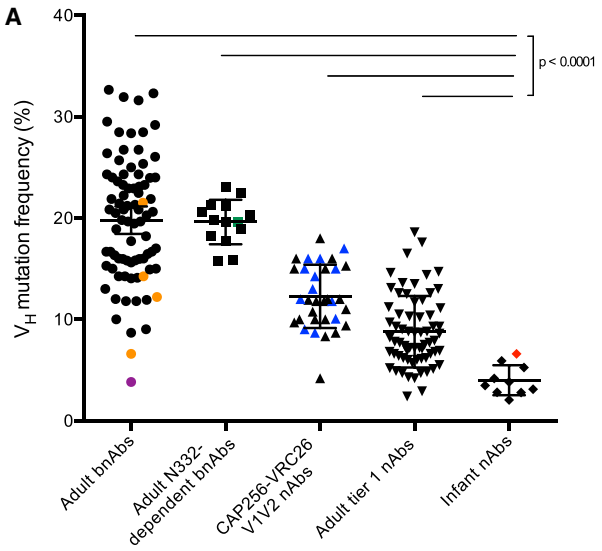

Figure 7. Levels of nAb SHM

Adult bnAbs include all nAbs available from http://bnaber.org. Yellow indicates first generation bnAbs. Purple indicates M66.6. V3 bnAbs include PGT120s, PGT130s, and 2G12. Green indicates PGT121. CAP256-VRC26 nAbs with >30% neutralization breadth are shown in blue. Adult tier 1 nAbs have limited tier 2 neutralizing activity. The cross-clade infant nAb BF520.1 is shown in red. Horizontal bars indicate mean and 95% confidence intervals. Mann-Whitney U test comparing infant nAb SHM to adult Nabs.
See also Figure S7.

B

	V-gene	D-gene	J-gene	CDRH3 length (AA)	VH mut frequency (nt)	VH indels (AA)	V-gene	J-gene	VL mut frequency (nt)	VL indels (AA)
PGT121	V4-59	D3-3	J6	26	20		LV3-21	LJ3	19	-7 (FR1)/ +3 (FR3)
PGT128	V4-39	D3-10	J5	21	20	+6 (CDR2)	LV2-8	LJ2	9	-5 (CDR1)
PGT135	V4-39	D3-9	J5	20	19	+5 (CDR1)	KV3-15	KJ1	18	
2G12	V3-21	D1-26	J3	16	21		KV1-5	KJ1	14	
BF520.1	V1-2	D3-10	J4	20	7		KV3-15	KJ3	5	

20 μl of culture supernatant was incubated for 1 hr at 37°C with ~325 infectious pseudovirus particles in 20 μl. Next, 3,000 TZM-bl cells in 20 μl DMEM plus 10% FBS and 1× PSF, GIBCO (1.5 × 10^5 cells ml^{-1}) and diethylaminoethyl (DEAE) dextran (10 μg ml^{-1} final concentration) were added to each well and cultured 37°C in a CO_2 incubator for 48 hr. β-galactosidase levels were measured using the Gal-Screen system (ThermoScientific). Briefly, 30 μl was removed from each well, 25 μl of substrate diluted 1:25 was added, incubated for 40 min at room temperature (RT), and read using a luminometer. Wells demonstrating >40% neutralization of one or both viruses were selected for RT-PCR amplification of the variable regions of the IgG heavy chain and kappa and lambda light chains, which were cloned into IgG expression vectors as previously described (Williams et al., 2015) with a modified RT step (Scherer et al., 2014).

Paired heavy and light chain plasmids cloned from the same well were co-transfected in equal ratios into 293F cells using the FreeStyle MAX system (Invitrogen). IgG was purified as described (Scherer et al., 2014). We screened 82 individual wells, from which 22 functional antibodies were produced.

Pseudovirus Production and Neutralization Assays

Methods for making pseudoviruses and performing neutralization assays using the TZM-bl system were as previously described (Goo et al., 2012b). Plasma IC_{50} values are the reciprocal plasma dilution resulting in 50% reduction of virus infectivity. Monoclonal antibody (mAb) IC_{50} values represent the mAb concentration in μg ml^{-1} at which 50% of the virus was neutralized. Reported IC_{50} values are the average of two or three independent experiments performed in duplicate.

Epitope Mapping

To screen for N332 nAbs, we compared neutralization of a clade A wild-type virus Q23.17 and a clade C wild-type virus DU156.12 to that of N332A mutants (Cortez et al., 2015) and a clade A wild-type virus BG505.W6.C2 (Wu et al., 2006) to that of a T332N mutant (Sanders et al., 2013). PGT128 and VRC01 were used as positive and negative controls, respectively (Walker et al., 2011; Wu et al., 2010). Reported IC_{50} values are the average of two independent experiments performed in duplicate.

Comparison of Infant nAb Activity to Adult bnAbs

Adult bnAbs b12, 2G12, 2F5 PG16, PGT151, and 10E8 were obtained from the NIH AIDS Reagent Program (Falkowska et al., 2014; West et al., 2014). All adult and infant antibody concentrations were determined by protein absorbance at 280 nm (Nanodrop). Heavy and light chain sequences for adult bnAbs VRC01, PGT121, PGT145 (West et al., 2014) were codon-optimized and synthesized (https://www.idtdna.com/site) and then cloned into the corresponding Igγ1, Igκ, and Igλ expression vectors and expressed and purified by the same method used for infant nAbs.

Somatic Hypermutation Analysis

Heavy and light chain sequences for adult bnAbs were obtained from http://bnaber.org (Eroshkin et al., 2014) or GenBank (Benson et al., 2005). Sequences were analyzed using IMGT V-QUEST (Lefranc et al., 2009) with percent SHM calculated as the VH mutation frequency at the nucleotide level. All sequences for adult nAbs with limited tier 2 neutralizing activity (Li et al., 2015) were obtained from GenBank. Sequences for recently published CAP256-VRC26 lineage antibodies (CAP256-VRC26.13-33) (Doria-Rose et al., 2015) were not available and published values were used for percent mutation from germline at the nucleotide level. Groups were compared using the Mann-Whitney U test performed using GraphPad Prism 9.0.

Cell-Surface Binding Assays

Binding to cell-surface Env was measured using a flow cytometry-based assay (Lovelace et al., 2011). 293T cells (3 × 10^6 cells) were transfected with 4 μg of HIV-1 env DNA using Fugene6 (Promega), harvested 48 hr post-transfection, and incubated with 20 μg ml^{-1} mAb. Next, cells were incubated with a 1:100 dilution of goat-anti-human IgG-PE (Santa Cruz), subsequently fixed with 1% paraformaldehyde, and processed by flow cytometry using a BD FACSCanto II. Data was analyzed using FlowJo software. Percent binding was calculated as the percentage of PE positive cells with background (mAb binding to mock transfected cells) subtracted. PGT128, BF520.3, BF520.4, and BF520.6 demonstrated >10% binding to mock transfected cells. Analyses were performed in GraphPad Prism 9.0.

SOSIP Production and Purification

Constructs encoding codon optimized BG505.W6.C2 T332N gp120 and SOSIP trimer (Sanders et al., 2013) as well as MG505.W0.E1 D295N I297T T332N were kindly provided by John Moore and colleagues and reverted to wild-type sequences using site-directed mutagenesis (Agilent) while retaining SOSIP modification (tPa signal peptide, furin cleavage site, I559P, A501C, and

T605C). A new SOSIP trimer was designed based on the Env sequence of BF520.W14.E3 and synthesized as a codon-optimized gene. A mAb-independent approach for purifying native-like SOSIP trimers was employed (manuscript in preparation). In brief, following production in 293F cells, soluble envelope oligomers were separated from the extracellular milieu using *Galanthus nivalis* lectin (Vector Labs). This mixture was then subjected to DEAE cation-exchange chromatography and trimer was resolved from aberrantly disulfide-bonded dimer and gp140 monomer using hydrophobic interaction chromatography and preparative grade size exclusion chromatography. Purity was assessed by SDS-PAGE, BN-PAGE, and dynamic light scattering and found to be >95% native-like trimer. Presence of native-like SOSIP trimer was further confirmed by negative-stain electron microscopy.

Fab Fragment Preparation

Fab fragments were generated from 500 μg of IgG antibody using a papain digestion kit (Pierce) and separated from Fc fragments and undigested IgG using a Protein A column (Pierce). Purity and size of Fab fragments was confirmed for six of ten antibodies by SDS-PAGE and mass spectrometry. The remaining four antibodies appeared to have been incompatible with papain digestion for Fab isolation from IgG and were not used for subsequent studies.

Kinetic Antibody Binding Assay by Octet Biolayer Interferometry

Binding kinetics of infant antibodies and Fab fragments with SOSIP trimers were determined using biolayer interferometry (BLI) on an Octet RED system (FortéBio). Hydrated anti-human IgG Fc Capture (AHC) or anti-human Fab-CH1 biosensors were immobilized for 4 min with purified infant antibodies diluted to 10 μg mL^{-1} in PBS (pH 7.4) supplemented with 1% BSA, 0.01% TWEEN 20, 0.02% sodium azide. After a stable baseline signal was established, antibody-immobilized tips were moved to wells containing a 2-fold dilution series of Env SOSIP trimer to monitor association for 4 min. Tips were then moved back to wells containing buffer to monitor dissociation for 15 min. Kinetics data were analyzed using FortéBio's Data Analysis 7.0. Average measurements from reference wells were subtracted and data were processed by Savitzky-Golay filtering prior to fitting using a 1:1 binding model. Reported kinetic constants are the average of 2 or 3 experiments using independent Env dilution series except in cases where dissociation was too minimal to be fit by the software.

Electron Microscopy

A 3-μl aliquot of BG505.W6.C2.T332N-BF520.1 complex, diluted to 20 μg ml^{-1} in PBS, was applied for 60 s to glow discharged C-Flat, 300 mesh, Cu grids (Electron Microscopy Sciences) and stained for an additional 60 s using Nano-W (Nanoprobes). Data were collected using a FEI Tecnai T12 transmission electron microscope operating at 120 keV. Images were taken using a Gatan 4 k × 4 k charge-coupled device (CCD) at a magnification of 52,000× and defocus range of 0.5–3.0 μm corresponding to a pixel size of 2.07 Å. Single particle reconstruction was performed using EMAN2.1 image processing suite (Tang et al., 2007). In short, particles were selected using interactive particle picking from 392 micrographs. A 2× binned, phase-flipped, CTF-corrected stack of 35,914 particles were created and subjected to reference free 2D classification and clustering to generate 200 2D classes. Classes containing free BF520.1-Fab or sub-stoichiometric populations were omitted, and the remaining 26,013 particles were reclassified to generate 150 2D classes. Again, classes containing sub-stoichiometric and free BF520.1-Fab populations were removed and a 2× binned particle stack containing 18,325 particles was used for 3D refinement using the coordinates from the PDB: 5ACO cryo-EM structure of BG505 SOSIP.664 HIV-1 Env trimer bound by PGT128 Fab (Lee et al., 2015). The model was low-pass filtered to 60 Å and used as an initial model for refinement with C3 symmetry imposed. Notably, the 5ACO coordinates only include the Fv and not the constant region of the PGT128 Fab; thus, the density we observe for the complete Fab emerged in the course of the reconstruction. The BG505 SOSIP-664 HIV-1 trimer (PDB: 4ZMJ) (Kwon et al., 2015) and PGT128-Fab crystal structure (PDB: 3TV3) (Pejchal et al., 2011) were docked into the negative-stained 3D map using UCSF Chimera package from the Computer Graphics Laboratory, University of California, San Francisco (Pettersen et al., 2004).

HIV-1 *env* Amplification and Cloning

Full-length *envs* were cloned from DNA isolated from uncultured PBMCs for the BF520 14-week (3.8 month) time point as previously described (Milligan et al., 2016). For the 6-month time point, *envs* were cloned total RNA that was extracted from 50 μl of plasma as described in Palmer et al. (2005). cDNA synthesis and nested PCR of full-length *env* was performed as previously described with minor modifications to the primers, which are available upon request (Milligan et al., 2016; Wu et al., 2006).

Phylogenetic Tree Analysis

Maternal (Milligan et al., 2016) and infant *env* sequences were aligned using MacClade version 4.01. A maximum likelihood phylogenetic tree was constructed using the HIV LANL HIV tools database PHYML interface (Guindon et al., 2010) (http://www.hiv.lanl.gov/content/sequence/PHYML/interface.html).

ACCESSION NUMBERS

The accession numbers for the Infant nAb sequences reported in this paper are GenBank: KX159304–KX159315 and KX168062–KX168069. The accession number for the maternal and infant HIV-1 envs reported in this paper is GenBank: KX168070–KX168123. The accession number for the EM density map reported in this paper is EMDataBank: EMD-8168.

SUPPLEMENTAL INFORMATION

Supplemental Information includes seven figures and can be found with this article online at http://dx.doi.org/10.1016/j.cell.2016.05.055.

AUTHOR CONTRIBUTIONS

J.O. conceived the study. J.O., C.A.S., K.L.W., H.P.V., J.A.W., and K.K.L. all contributed to the design of the study. C.A.S., K.L.W., H.P.V., and J.A.W. performed experiments. R.N. developed the cohort and collected samples. All authors contributed to the analysis and interpretation of data. C.A.S., K.K.L., and J.O. wrote the manuscript with input from all authors.

ACKNOWLEDGMENTS

We thank the participants and staff of the Nairobi Breastfeeding Trial. We are grateful to Justin Taylor for helpful discussions regarding flow cytometry, John McNevin for help with cell sorting, Stephanie Rainwater and Brianna Hennessy for assistance preparing pseudoviruses and constructing BF520 envelope clones, Stanley Riddell for providing 3T3/CD40L cells, and David Veesler for advice regarding analysis of EM data. Panel of Global HIV-1 Env Clones (cat# 12670) was obtained through the NIH AIDS Reagent Program, Division of AIDS, NIAID, NIH from David Montefiori. This work was supported by NIH grants R01 AI076105, R01 AI103981, R01 AI120961, R21 AI112389, F30 AI122866, and T32 AI083203.

Received: March 5, 2016
Revised: April 19, 2016
Accepted: May 17, 2016
Published: June 23, 2016

REFERENCES

Benson, D.A., Karsch-Mizrachi, I., Lipman, D.J., Ostell, J., and Wheeler, D.L. (2005). GenBank. Nucleic Acids Res. *33*, D34–D38.

Burton, D.R., and Mascola, J.R. (2015). Antibody responses to envelope glycoproteins in HIV-1 infection. Nat. Immunol. *16*, 571–576.

Cortez, V., Wang, B., Dingens, A., Chen, M.M., Ronen, K., Georgiev, I.S., McClelland, R.S., and Overbaugh, J. (2015). The broad neutralizing antibody responses after HIV-1 superinfection are not dominated by antibodies directed to epitopes common in single infection. PLoS Pathog. *11*, e1004973.

deCamp, A., Hraber, P., Bailer, R.T., Seaman, M.S., Ochsenbauer, C., Kappes, J., Gottardo, R., Edlefsen, P., Self, S., Tang, H., et al. (2014). Global panel of HIV-1 Env reference strains for standardized assessments of vaccine-elicited neutralizing antibodies. J. Virol. *88*, 2489–2507.

Doria-Rose, N.A., and Joyce, M.G. (2015). Strategies to guide the antibody affinity maturation process. Curr. Opin. Virol. *11*, 137–147.

Doria-Rose, N.A., Schramm, C.A., Gorman, J., Moore, P.L., Bhiman, J.N., DeKosky, B.J., Ernandes, M.J., Georgiev, I.S., Kim, H.J., Pancera, M., et al.; NISC Comparative Sequencing Program (2014). Developmental pathway for potent V1V2-directed HIV-neutralizing antibodies. Nature *509*, 55–62.

Doria-Rose, N.A., Bhiman, J.N., Roark, R.S., Schramm, C.A., Gorman, J., Chuang, G.Y., Pancera, M., Cale, E.M., Ernandes, M.J., Louder, M.K., et al. (2015). New member of the V1V2-directed CAP256-VRC26 lineage that shows increased breadth and exceptional potency. J. Virol. *90*, 76–91.

Eroshkin, A.M., LeBlanc, A., Weekes, D., Post, K., Li, Z., Rajput, A., Butera, S.T., Burton, D.R., and Godzik, A. (2014). bNAber: database of broadly neutralizing HIV antibodies. Nucleic Acids Res. *42*, D1133–D1139.

Falkowska, E., Le, K.M., Ramos, A., Doores, K.J., Lee, J.H., Blattner, C., Ramirez, A., Derking, R., van Gils, M.J., Liang, C.H., et al. (2014). Broadly neutralizing HIV antibodies define a glycan-dependent epitope on the prefusion conformation of gp41 on cleaved envelope trimers. Immunity *40*, 657–668.

Fouts, T.R., Binley, J.M., Trkola, A., Robinson, J.E., and Moore, J.P. (1997). Neutralization of the human immunodeficiency virus type 1 primary isolate JR-FL by human monoclonal antibodies correlates with antibody binding to the oligomeric form of the envelope glycoprotein complex. J. Virol. *71*, 2779–2785.

Goo, L., Jalalian-Lechak, Z., Richardson, B.A., and Overbaugh, J. (2012a). A combination of broadly neutralizing HIV-1 monoclonal antibodies targeting distinct epitopes effectively neutralizes variants found in early infection. J. Virol. *86*, 10857–10861.

Goo, L., Milligan, C., Simonich, C.A., Nduati, R., and Overbaugh, J. (2012b). Neutralizing antibody escape during HIV-1 mother-to-child transmission involves conformational masking of distal epitopes in envelope. J. Virol. *86*, 9566–9582.

Goo, L., Chohan, V., Nduati, R., and Overbaugh, J. (2014). Early development of broadly neutralizing antibodies in HIV-1-infected infants. Nat. Med. *20*, 655–658.

Guindon, S., Dufayard, J.F., Lefort, V., Anisimova, M., Hordijk, W., and Gascuel, O. (2010). New algorithms and methods to estimate maximum-likelihood phylogenies: assessing the performance of PhyML 3.0. Syst. Biol. *59*, 307–321.

Haigwood, N.L., Montefiori, D.C., Sutton, W.F., McClure, J., Watson, A.J., Voss, G., Hirsch, V.M., Richardson, B.A., Letvin, N.L., Hu, S.L., and Johnson, P.R. (2004). Passive immunotherapy in simian immunodeficiency virus-infected macaques accelerates the development of neutralizing antibodies. J. Virol. *78*, 5983–5995.

Hoot, S., McGuire, A.T., Cohen, K.W., Strong, R.K., Hangartner, L., Klein, F., Diskin, R., Scheid, J.F., Sather, D.N., Burton, D.R., and Stamatatos, L. (2013). Recombinant HIV envelope proteins fail to engage germline versions of anti-CD4bs bNAbs. PLoS Pathog. *9*, e1003106.

Huang, J., Doria-Rose, N.A., Longo, N.S., Laub, L., Lin, C.L., Turk, E., Kang, B.H., Migueles, S.A., Bailer, R.T., Mascola, J.R., and Connors, M. (2013). Isolation of human monoclonal antibodies from peripheral blood B cells. Nat. Protoc. *8*, 1907–1915.

Jardine, J.G., Ota, T., Sok, D., Pauthner, M., Kulp, D.W., Kalyuzhniy, O., Skog, P.D., Thinnes, T.C., Bhullar, D., Briney, B., et al. (2015). HIV-1 VACCINES. Priming a broadly neutralizing antibody response to HIV-1 using a germline-targeting immunogen. Science *349*, 156–161.

Kepler, T.B., Liao, H.X., Alam, S.M., Bhaskarabhatla, R., Zhang, R., Yandava, C., Stewart, S., Anasti, K., Kelsoe, G., Parks, R., et al. (2014). Immunoglobulin gene insertions and deletions in the affinity maturation of HIV-1 broadly reactive neutralizing antibodies. Cell Host Microbe *16*, 304–313.

Klein, F., Diskin, R., Scheid, J.F., Gaebler, C., Mouquet, H., Georgiev, I.S., Pancera, M., Zhou, T., Incesu, R.B., Fu, B.Z., et al. (2013a). Somatic mutations of the immunoglobulin framework are generally required for broad and potent HIV-1 neutralization. Cell *153*, 126–138.

Klein, F., Mouquet, H., Dosenovic, P., Scheid, J.F., Scharf, L., and Nussenzweig, M.C. (2013b). Antibodies in HIV-1 vaccine development and therapy. Science *341*, 1199–1204.

Kong, L., Lee, J.H., Doores, K.J., Murin, C.D., Julien, J.P., McBride, R., Liu, Y., Marozsan, A., Cupo, A., Klasse, P.J., et al. (2013). Supersite of immune vulnerability on the glycosylated face of HIV-1 envelope glycoprotein gp120. Nat. Struct. Mol. Biol. *20*, 796–803.

Kunert, R., Rüker, F., and Katinger, H. (1998). Molecular characterization of five neutralizing anti-HIV type 1 antibodies: identification of nonconventional D segments in the human monoclonal antibodies 2G12 and 2F5. AIDS Res. Hum. Retroviruses *14*, 1115–1128.

Kwon, Y.D., Pancera, M., Acharya, P., Georgiev, I.S., Crooks, E.T., Gorman, J., Joyce, M.G., Guttman, M., Ma, X., Narpala, S., et al. (2015). Crystal structure, conformational fixation and entry-related interactions of mature ligand-free HIV-1 Env. Nat. Struct. Mol. Biol. *22*, 522–531.

Landais, E., Huang, X., Havenar-Daughton, C., Murrell, B., Price, M.A., Wickramasinghe, L., Ramos, A., Bian, C.B., Simek, M., Allen, S., et al. (2016). Broadly neutralizing antibody responses in a large longitudinal sub-saharan HIV primary infection cohort. PLoS Pathog. *12*, e1005369.

Lee, J.H., de Val, N., Lyumkis, D., and Ward, A.B. (2015). Model building and refinement of a natively glycosylated HIV-1 Env protein by high-resolution cryoelectron microscopy. Structure *23*, 1943–1951.

Lefranc, M.P., Giudicelli, V., Ginestoux, C., Jabado-Michaloud, J., Folch, G., Bellahcene, F., Wu, Y., Gemrot, E., Brochet, X., Lane, J., et al. (2009). IMGT, the international ImMunoGeneTics information system. Nucleic Acids Res. *37*, D1006–D1012.

Li, L., Wang, X.H., Williams, C., Volsky, B., Steczko, O., Seaman, M.S., Luthra, K., Nyambi, P., Nadas, A., Giudicelli, V., et al. (2015). A broad range of mutations in HIV-1 neutralizing human monoclonal antibodies specific for V2, V3, and the CD4 binding site. Mol. Immunol. *66*, 364–374.

Liao, H.X., Lynch, R., Zhou, T., Gao, F., Alam, S.M., Boyd, S.D., Fire, A.Z., Roskin, K.M., Schramm, C.A., Zhang, Z., et al.; NISC Comparative Sequencing Program (2013). Co-evolution of a broadly neutralizing HIV-1 antibody and founder virus. Nature *496*, 469–476.

Lovelace, E., Xu, H., Blish, C.A., Strong, R., and Overbaugh, J. (2011). The role of amino acid changes in the human immunodeficiency virus type 1 transmembrane domain in antibody binding and neutralization. Virology *421*, 235–244.

Lynch, R.M., Boritz, E., Coates, E.E., DeZure, A., Madden, P., Costner, P., Enama, M.E., Plummer, S., Holman, L., Hendel, C.S., et al.; VRC 601 Study Team (2015). Virologic effects of broadly neutralizing antibody VRC01 administration during chronic HIV-1 infection. Sci. Transl. Med. *7*, 319ra206.

Mascola, J.R., and Haynes, B.F. (2013). HIV-1 neutralizing antibodies: understanding nature's pathways. Immunol. Rev. *254*, 225–244.

Milligan, C., Omenda, M.M., Chohan, V., Odem-Davis, K., Richardson, B.A., Nduati, R., and Overbaugh, J. (2016). Maternal neutralization-resistant virus variants do not predict infant HIV infection risk. MBio *7*, e02221–15.

Moody, M.A., Yates, N.L., Amos, J.D., Drinker, M.S., Eudailey, J.A., Gurley, T.C., Marshall, D.J., Whitesides, J.F., Chen, X., Foulger, A., et al. (2012). HIV-1 gp120 vaccine induces affinity maturation in both new and persistent antibody clonal lineages. J. Virol. *86*, 7496–7507.

Mouquet, H. (2014). Antibody B cell responses in HIV-1 infection. Trends Immunol. *35*, 549–561.

Mouquet, H., Scharf, L., Euler, Z., Liu, Y., Eden, C., Scheid, J.F., Halper-Stromberg, A., Gnanapragasam, P.N., Spencer, D.I., Seaman, M.S., et al. (2012). Complex-type N-glycan recognition by potent broadly neutralizing HIV antibodies. Proc. Natl. Acad. Sci. USA *109*, E3268–E3277.

Nduati, R., John, G., Mbori-Ngacha, D., Richardson, B., Overbaugh, J., Mwatha, A., Ndinya-Achola, J., Bwayo, J., Onyango, F.E., Hughes, J., and Kreiss, J.

(2000). Effect of breastfeeding and formula feeding on transmission of HIV-1: a randomized clinical trial. JAMA *283*, 1167–1174.

Ng, C.T., Jaworski, J.P., Jayaraman, P., Sutton, W.F., Delio, P., Kuller, L., Anderson, D., Landucci, G., Richardson, B.A., Burton, D.R., et al. (2010). Passive neutralizing antibody controls SHIV viremia and enhances B cell responses in infant macaques. Nat. Med. *16*, 1117–1119.

Palmer, S., Kearney, M., Maldarelli, F., Halvas, E.K., Bixby, C.J., Bazmi, H., Rock, D., Falloon, J., Davey, R.T., Jr., Dewar, R.L., et al. (2005). Multiple, linked human immunodeficiency virus type 1 drug resistance mutations in treatment-experienced patients are missed by standard genotype analysis. J. Clin. Microbiol. *43*, 406–413.

Parren, P.W., Mondor, I., Naniche, D., Ditzel, H.J., Klasse, P.J., Burton, D.R., and Sattentau, Q.J. (1998). Neutralization of human immunodeficiency virus type 1 by antibody to gp120 is determined primarily by occupancy of sites on the virion irrespective of epitope specificity. J. Virol. *72*, 3512–3519.

Pejchal, R., Doores, K.J., Walker, L.M., Khayat, R., Huang, P.S., Wang, S.K., Stanfield, R.L., Julien, J.P., Ramos, A., Crispin, M., et al. (2011). A potent and broad neutralizing antibody recognizes and penetrates the HIV glycan shield. Science *334*, 1097–1103.

Pettersen, E.F., Goddard, T.D., Huang, C.C., Couch, G.S., Greenblatt, D.M., Meng, E.C., and Ferrin, T.E. (2004). UCSF Chimera–a visualization system for exploratory research and analysis. J. Comput. Chem. *25*, 1605–1612.

Sanders, R.W., Derking, R., Cupo, A., Julien, J.P., Yasmeen, A., de Val, N., Kim, H.J., Blattner, C., de la Peña, A.T., Korzun, J., et al. (2013). A next-generation cleaved, soluble HIV-1 Env trimer, BG505 SOSIP.664 gp140, expresses multiple epitopes for broadly neutralizing but not non-neutralizing antibodies. PLoS Pathog. *9*, e1003618.

Sanders, R.W., van Gils, M.J., Derking, R., Sok, D., Ketas, T.J., Burger, J.A., Ozorowski, G., Cupo, A., Simonich, C., Goo, L., et al. (2015). HIV-1 VACCINES. HIV-1 neutralizing antibodies induced by native-like envelope trimers. Science *349*, aac4223.

Scanlan, C.N., Pantophlet, R., Wormald, M.R., Ollmann Saphire, E., Stanfield, R., Wilson, I.A., Katinger, H., Dwek, R.A., Rudd, P.M., and Burton, D.R. (2002). The broadly neutralizing anti-human immunodeficiency virus type 1 antibody 2G12 recognizes a cluster of alpha1–>2 mannose residues on the outer face of gp120. J. Virol. *76*, 7306–7321.

Scheid, J.F., Mouquet, H., Ueberheide, B., Diskin, R., Klein, F., Oliveira, T.Y., Pietzsch, J., Fenyo, D., Abadir, A., Velinzon, K., et al. (2011). Sequence and structural convergence of broad and potent HIV antibodies that mimic CD4 binding. Science *333*, 1633–1637.

Scherer, E.M., Smith, R.A., Simonich, C.A., Niyonzima, N., Carter, J.J., and Galloway, D.A. (2014). Characteristics of memory B cells elicited by a highly efficacious HPV vaccine in subjects with no pre-existing immunity. PLoS Pathog. *10*, e1004461.

Siegrist, C.A., and Aspinall, R. (2009). B-cell responses to vaccination at the extremes of age. Nat. Rev. Immunol. *9*, 185–194.

Sok, D., Laserson, U., Laserson, J., Liu, Y., Vigneault, F., Julien, J.P., Briney, B., Ramos, A., Saye, K.F., Le, K., et al. (2013). The effects of somatic hypermutation on neutralization and binding in the PGT121 family of broadly neutralizing HIV antibodies. PLoS Pathog. *9*, e1003754.

Tang, G., Peng, L., Baldwin, P.R., Mann, D.S., Jiang, W., Rees, I., and Ludtke, S.J. (2007). EMAN2: an extensible image processing suite for electron microscopy. J. Struct. Biol. *157*, 38–46.

Trkola, A., Purtscher, M., Muster, T., Ballaun, C., Buchacher, A., Sullivan, N., Srinivasan, K., Sodroski, J., Moore, J.P., and Katinger, H. (1996). Human monoclonal antibody 2G12 defines a distinctive neutralization epitope on the gp120 glycoprotein of human immunodeficiency virus type 1. J. Virol. *70*, 1100–1108.

Walker, L.M., Huber, M., Doores, K.J., Falkowska, E., Pejchal, R., Julien, J.P., Wang, S.K., Ramos, A., Chan-Hui, P.Y., Moyle, M., et al.; Protocol G Principal Investigators (2011). Broad neutralization coverage of HIV by multiple highly potent antibodies. Nature *477*, 466–470.

West, A.P., Jr., Scharf, L., Scheid, J.F., Klein, F., Bjorkman, P.J., and Nussenzweig, M.C. (2014). Structural insights on the role of antibodies in HIV-1 vaccine and therapy. Cell *156*, 633–648.

Wibmer, C.K., Moore, P.L., and Morris, L. (2015). HIV broadly neutralizing antibody targets. Curr. Opin. HIV AIDS *10*, 135–143.

Williams, K.L., Cortez, V., Dingens, A.S., Gach, J.S., Rainwater, S., Weis, J.F., Chen, X., Spearman, P., Forthal, D.N., and Overbaugh, J. (2015). HIV-specific CD4-induced antibodies mediate broad and potent antibody-dependent cellular cytotoxicity activity and are commonly detected in plasma from HIV-infected humans. EBioMedicine *2*, 1464–1477.

Wu, X., Parast, A.B., Richardson, B.A., Nduati, R., John-Stewart, G., Mbori-Ngacha, D., Rainwater, S.M., and Overbaugh, J. (2006). Neutralization escape variants of human immunodeficiency virus type 1 are transmitted from mother to infant. J. Virol. *80*, 835–844.

Wu, X., Yang, Z.Y., Li, Y., Hogerkorp, C.M., Schief, W.R., Seaman, M.S., Zhou, T., Schmidt, S.D., Wu, L., Xu, L., et al. (2010). Rational design of envelope identifies broadly neutralizing human monoclonal antibodies to HIV-1. Science *329*, 856–861.

Yasmeen, A., Ringe, R., Derking, R., Cupo, A., Julien, J.P., Burton, D.R., Ward, A.B., Wilson, I.A., Sanders, R.W., Moore, J.P., and Klasse, P.J. (2014). Differential binding of neutralizing and non-neutralizing antibodies to native-like soluble HIV-1 Env trimers, uncleaved Env proteins, and monomeric subunits. Retrovirology *11*, 41.

Yu, L., and Guan, Y. (2014). Immunologic basis for long HCDR3s in broadly neutralizing antibodies against HIV-1. Front. Immunol. *5*, 250.

Zhou, T., Georgiev, I., Wu, X., Yang, Z.Y., Dai, K., Finzi, A., Kwon, Y.D., Scheid, J.F., Shi, W., Xu, L., et al. (2010). Structural basis for broad and potent neutralization of HIV-1 by antibody VRC01. Science *329*, 811–817.

Zhu, Z., Qin, H.R., Chen, W., Zhao, Q., Shen, X., Schutte, R., Wang, Y., Ofek, G., Streaker, E., Prabakaran, P., et al. (2011). Cross-reactive HIV-1-neutralizing human monoclonal antibodies identified from a patient with 2F5-like antibodies. J. Virol. *85*, 11401–11408.